Influence of complex terrain on a flow above a forest with clearing

Influence of complex terrain on a flow above a forest with clearing

Influence of complex terrain on a flow above a forest with clearing

Johanna Matsfelt[1], Lars Davidson[1], Kyle Brennan[2]

[1] Division of Fluid Dynamics, Department of Mechanics and Maritime Sciences, Gothenburg, SE-412 96, Sweden

[2] Meventus AS, Kongsgård Allé 59, 4630 Kristiansand S, Norway

E-mail: johanna.matsfelt@chalmers.se

Abstract.

Large Eddy simulations of the Lemnhult wind farm in Sweden are compared to LiDAR measurements of the site.Two scans have been performed, one in southerly direction in order to investigate the flow over a forest, another one in westerly direction, in order to investigate the flow over a clearing. A forest model is implemented in STAR-CCM+ using the local forest height data, while assuming flat terrain in one simulation and including the terrain height in another to investigate its effect for each scan. The complex terrain simulations show the best agreement with the measurements. Uncertainty of the stratification of the measurements can be the reason for some of the difference. The vertical wind speed for the clearing scan change considerably when the terrain representation is included, but the magnitude is however still low compared to the horizontal velocity. This shows the importance of including terrain for simulations with variation in terrain height. The normalized turbulent kinetic energy for the vertical profiles show a decrease in the clearing scan compared to the forest scan which should be beneficial for wind turbines.

1. Introduction

Large areas in Sweden are covered by forest, conditions that have been proven to increase turbulence above the IEC design criteria [1]. When the turbulence increase above these criteria the fatigue loads on the wind turbine increase and thereby also the maintenance cost making the wind turbines less profitable [2]. To study this in more detail, laser scanned forest and terrain height at a site are implemented in STAR-CCM+ and a comparison is made with and without terrain height and validated against LiDAR measurements.

Flow over a forest edge has been simulated and compared to measurements in [3] for two different forests with a leaf area index (LAI) of two and five. The forest with the highest LAI i.e. the densest forest showed the highest values of the total kinetic energy of the two forests. In both forests the total kinetic energy increased as the flow moved along the forest. Using a neutral stratified flow it has been showed in [4] using Reynolds Averaged Navier Stokes (RANS) and in [5] using Large Eddy Simulation (LES) that the scalar accumulation occurring downstream of a forest edge is partly due to the converging of the mean flow. In both papers the scalar flux concentration occurring downstream of the forest edge moved toward the forest edge as the LAI increased. The reason for this was the higher drag force for the more dense forest. In the

papers when the velocity decreased the concentration peak increased but the flux peak remained unchanged.

The distance affected by the forest edge has been investigated in numerous papers. In [6] edge effects were seen up to 22 forest heights after the forest edge. When the clearings are streamwise larger than five forest height the flow will always show edge effects because the formation of sub-canopy wind jet at the forest edges [7]. The shape of the clearing has been shown to change, and in some cases improve the flow field [8]. In [9] a clearing in form of a lake is studied. The wind shear was showed to be the main reason for the turbulent mixing rather than the thermal stratification due to the lake.

LES has been used to study complex terrain. In [7] a 2D forested hill was simulated using LES and validated against a wind tunnel experiment giving good agreement. In [10] two participants using LES took part of a study of simulating the wind profile at the Ryningsnäs wind farm in Sweden from tree different wind directions. Here an airborne laser scan was used to obtain the topology and the forest density given to the modellers. The LES with the larger domain and lowest resolution gave the best agreement to the measurements. An airborne laser scan was also used in [11] for a newly developed model and compared to the data provided by the Swedish Forest Agency. The two data sets showed good agreement and due to the data provided by the Swedish Forest Agency is continuously updated it was recommended by the authors.

2. Objectives

LES of the Lemnhult wind farm in Sweden including varying forest height with and without terrain height are compared to LiDAR measurement. To validate the simulation model two LiDAR scans are used, the west scan represents a clearing and the south scan represents forest.

3. Methodology

This article cover both the measurement campaign and the simulations at the Lemnhult wind farm.

3.1. Simulations

LES is used to simulate a flow under neutral stratification, the sub-grid model used in STAR-CCM+ is the WALE model [12]. To simulate the forest, a drag source is added to the transport equation of momentum [13].

$$F_{f,i} = -C_{Df} a_f U_h \bar{u}_i \tag{1}$$

$$U_h = \sqrt{U_1^2 + U_2^2} \tag{2}$$

In eq. 1 C_{Df} is set to 0.15 and is the drag coefficient of the forest [13]. U_h is the horizontal wind speed in eq. 2 is calculated using the two velocities in the horizontal plane and $\bar{u}_i$ is the velocity vector. To simulate the shape of the forest the vertical leaf density a_f is used, a representation can be seen in fig. 1.

The vertical leaf area density can be found by e.g. measuring it in the forest or by an empirical formula as has been done here [14, 10]. The n, L_m and z_m parameters in eq. 3 determine the shape of the forest. The kind of forest is determined by the L_m and z_m parameters [13, 14]. In this investigation scots pine trees are used with a z_m of $0.6h$, where h is the height of the forest and a L_m of 0.37 [13, 14]. The n parameter can be evaluated in different ways, here eq. 4 is used [14].

$$a_f(z) = L_m \left(\frac{h - z_m}{h - z}\right)^n \exp\left(n\left(1 - \left(\frac{h - z_m}{h - z}\right)\right)\right) \tag{3}$$

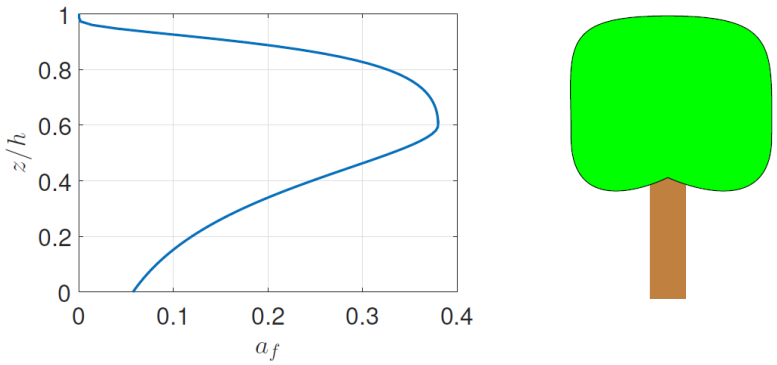

Figure 1. A representation of how the vertical leaf area density profile is used to simulate a tree.

$$n = \begin{cases} 6 & 0 \leq z < z_m, \\ \frac{1}{2} & z_m \leq z \leq h \end{cases} \tag{4}$$

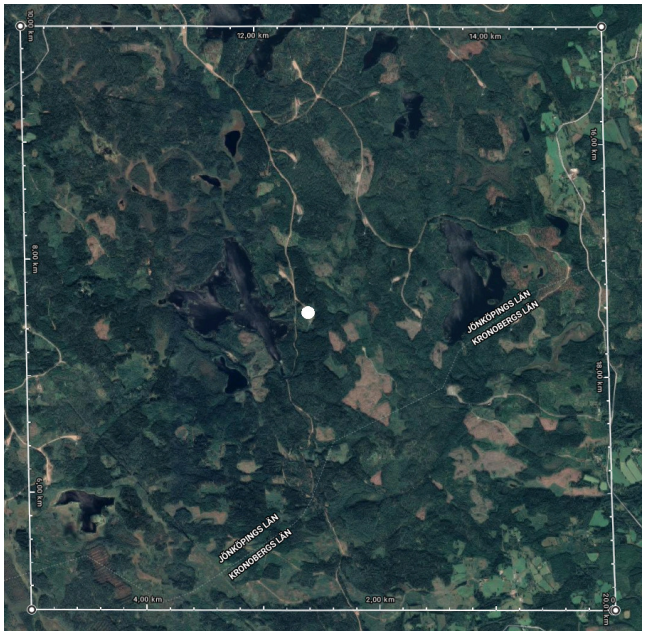

Figure 2. Satellite view of the simulated region with the location of the computational domain marked by a square. The location of the LiDAR in the middle marked by a white dot.

The simulation domain is 5000 m in each horizontal direction and 1000 m in the vertical direction. A satellite view of the domain can be seen in fig. 2. The horizontal mesh resolution is 4 m. The vertical mesh resolution is constant 2 m up to 200 m from the ground, after that it is stretched to 10 m at the top of the domain. The same mesh resolution is used in all the simulations. The inlet boundary condition is synthetic turbulence applied to a time-averaged velocity profile [15]. The turbulence is subscribed by a turbulence intensity of 10% and a length scale of 100 m. The time-averaged velocity inlet profile used has been developed over five flow passes. The time-averaged velocity field at the outlet plane is after each flow pass used as

Figure 3. Satellite view of the simulated region with the location of the computational domain marked by a square. The location of the LiDAR in the middle marked by a white dot.

time-averaged velocity inlet profile for the subsequent flow pass. The reason for this is to better represent the inlet to the computational domain from the surrounding seen in fig. 3 without the computational cost of a full precursor simulation. The outlet is specified as a pressure outlet. The top and sides of the computational domain is using symmetry boundary conditions.

The terrain and forest height at the location is taken from the Swedish Forest Agency with a 1 m resolution [16]. The terrain height is implemented as a surface which is used for creating the surface mesh. The forest height is implemented using an xyz file defining the local h parameter in eq. 3.

3.2. Measurements

The measurement campaign consisted of a Halo Photonics StreamLine XR LiDAR placed adjacent to the southwestern most turbine in the Lemnhult wind farm. The LiDAR and neighbor wind turbine are located in a small clearing in a generally forested area, with a small lake to the west. A neighbor wind farm approximately 2 km to the west of the LiDAR position and can be seen in the west limit of the computational domain marked in fig. 3.

The LiDAR was installed on a small hilltop approximately 28 m south of the adjacent turbine. The LiDAR was primarily run in 10 min stare in quads 1 and 2 seen in table 1 and depicted in fig. 4. The LiDAR was run in DBS feedback mode (Derived Bearing Scan), where the LiDAR measures the vertical wind profile after each programmed scan to determine the wind direction (or bearing). The resulting direction was resolved nearest the 129 m hub height of the neighbor wind turbine and used to select the corresponding scan based on the quadrants described in table 1.

The individual scan geometries were designed to keep the vertical angle as low as possible while ensuring clearance over local obstructions. This low vertical angle ensured the measurements were at or below hub height for most of the 2 km horizontal range of the LiDAR while also measuring at or near the forest canopy at positions closest to the LiDAR. The

Table 1. LiDAR measurement quads and descriptions.

Quad	Directions [degrees]	Description
1	145 to 220	Southern scan to measure flow over forest
2	220 to 320	Western scan to measure flow over clearing
3	320 to 40	Southern scan to measure wake over forest
4	40 to 145	Western scan to measure wake over clearing

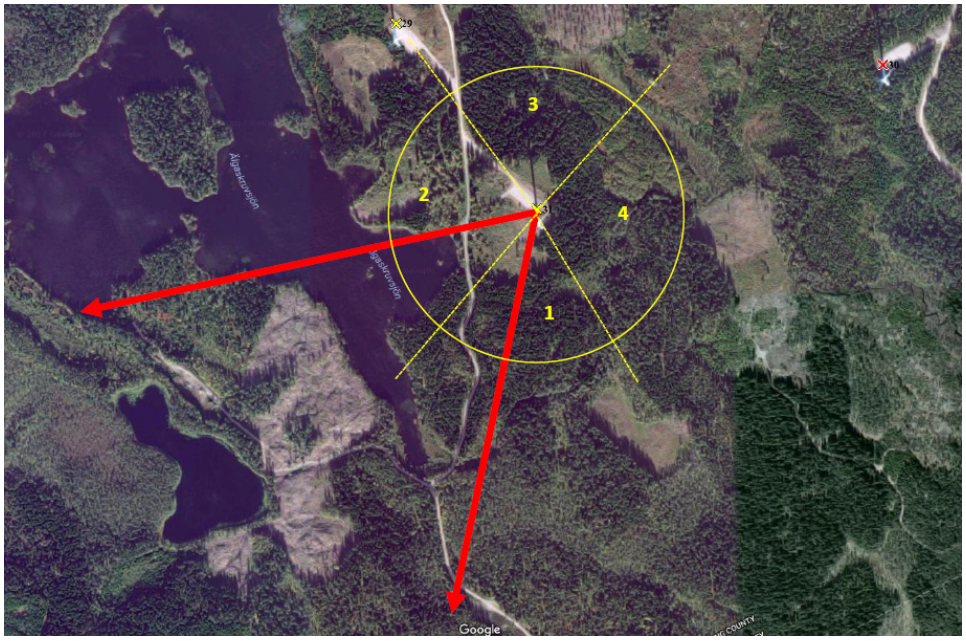

Figure 4. Directional quadrants to determine the LiDAR scan selection in DBS feedback mode.

directional azimuths were fine-tuned during installation based on the site conditions to ensure an unobstructed path for the laser. The resulting Southern scan had a horizontal azimuth of 191 degree magnetic (195 degree relative to True North) and vertical angle of 5 degrees. The Western scan had a horizontal azimuth of 253 degree magnetic (257 degree relative to True North) and vertical angle of 3.3 degrees. The LiDAR measurements were taken at 1Hz with range gates of 18 meters. A constant azimuth and elevation were retained for periods of 10 minutes in order to describe the temporal changes in the flow field. Installation photos depicting the scan geometries and the local terrain for both scans can be seen in figs. 5 and 6.

No measurements to evaluate the stratification are included in the measurement campaign. To increase the probability that the simulations are compared to measurements at neutral stratification, the measurements chosen is 10 min averaged at blowy, well mixed night conditions.

4. Results

Simulations are performed with and without complex terrain both for the west i.e. clearing scan and south i.e. forest scan and comparisons to the LiDAR scans are made. This is followed by a comparison of full vertical profiles at the location of the wind turbine.

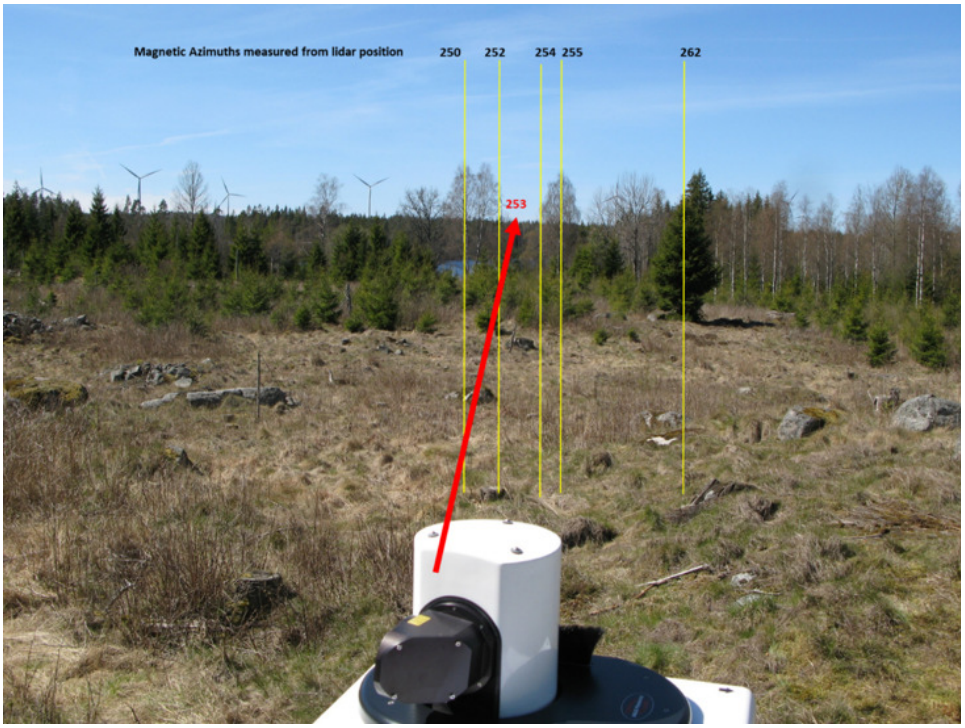

Figure 5. Western scan over the clearing geometry terrain and obstructions seen from LiDAR location.

4.1. LiDAR scan comparison

The predicted horizontal wind speed for the south scan, i.e. forest scan with and without terrain height, is compared to 10 min averaged LiDAR measurement and can be seen in fig. 7. The simulations and the LiDAR measurements show good agreement for the south scan.

The forest height and the terrain height for the south scan is shown in fig. 8 using the horizontal distance as distance measurement described by eq. 5.

$$x_h = \sqrt{x_1^2 + x_2^2} \tag{5}$$

By including the terrain height the result from the simulation is showing even better agreement. The uncertainty in the stratification of the LiDAR measurement can be the reason for some of the difference [17].

The horizontal wind speed from the simulation and the LiDAR measurement for the west scan, i.e. the clearing scan, can be seen in fig. 9. Also here the best agreement is for the simulation when the complex terrain is included. The forest height and the terrain height along the horizontal distance for the clearing scan can be seen in fig. 10. The horizontal wind speed is seen in fig. 11 plotted along the horizontal distance from the LiDAR position. The complex terrain simulation is predicting a bit lower velocity. Also the local max and min location of the velocity profile in the region of the clearing is shifted about 100 m away from the wind turbine. In the LiDAR measurements, only the maximum location can be measured, and it is located about 50 m in the direction away from the wind turbine compared to the simulation with complex terrain.

When the complex terrain is added the vertical wind speed seen in fig. 12 increases its local max and min, but the absolute value is still small compared to the horizontal wind speed. The turbulent kinetic energy seen in fig. 13 shows much lower values for the 175 m closest to the wind

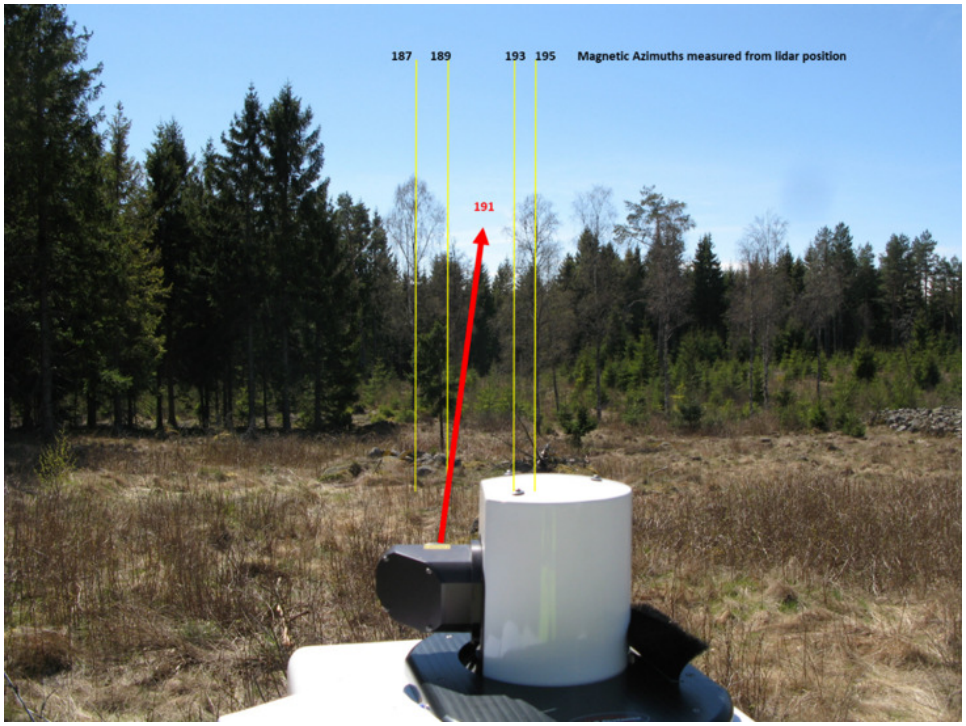

Figure 6. Southern scan over the clearing geometry terrain and obstructions seen from LiDAR location.

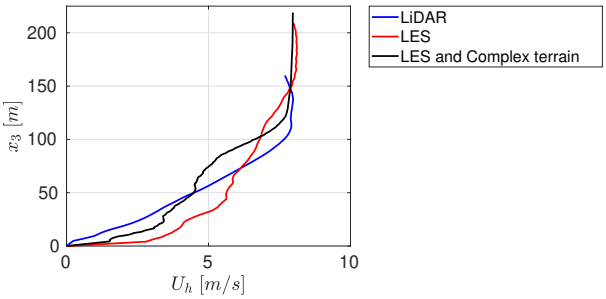

Figure 7. The horizontal wind speed for the south scan i.e. the forest scan. The LES data are extracted at the same location and height as the LiDAR measurements.

turbine. Further away from the wind turbine the shift between local max and min increases as the distance increases.

4.2. Vertical profiles

To compare the different simulations vertical profiles at the position of the wind turbine they are normalized with the horizontal wind speed at 750 m. When looking at the normalized horizontal wind speed in fig. 14 the difference between including the complex terrain or not is larger for the south scan (i.e. forest) compared to the west (i.e. clearing). The difference in terrain height 1 km from the wind turbine location is 10 m in the south scan compared to 7.5 m in the west scan. The fact that the clearing is a lake, i.e. it is flat, also decreases the impact of the terrain.

The normalized vertical wind speeds can be seen in fig. 15. They are normalized with the

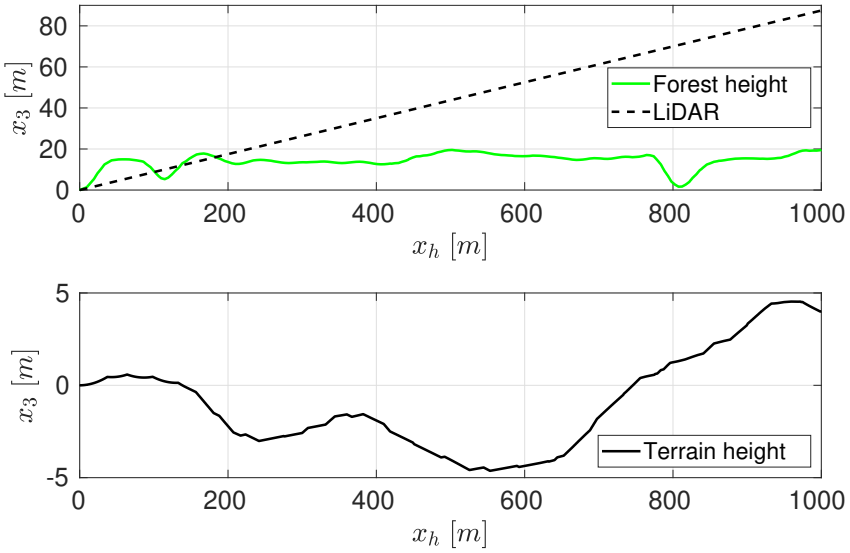

Figure 8. The top graph shows forest height and LiDAR height scan location from the location of the LiDAR for the south scan. The bottom graph displays the change in elevation.

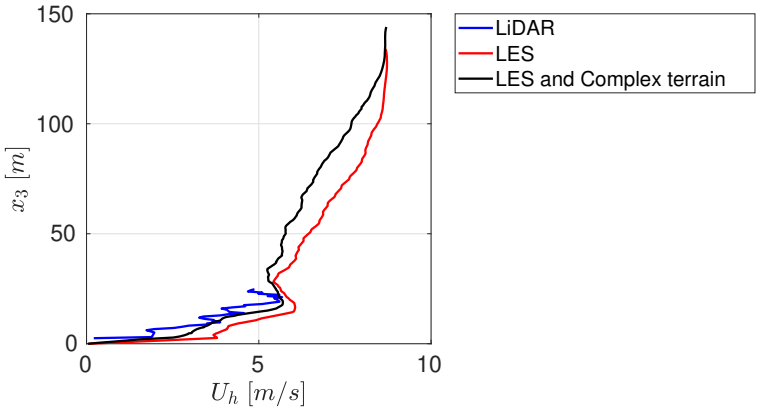

Figure 9. The horizontal wind speed for the west scan i.e. flow above a clearing. The LES data is extracted at the same location and height as the LiDAR measurements.

horizontal wind speed so the magnitude is very small. The south scan has somewhat similar shape when the complex terrain is introduced, despite having somewhat larger difference in terrain height 1 km from the wind turbine. When looking at the west scan the shape changes a lot when the complex terrain is introduced. This could be due to the increase in terrain height over the 300 m from the wind turbine seen in fig. 10.

The normalized turbulent kinetic energy (tke) is shown in fig. 16. The south scan i.e. above the forest mainly predicts a higher tke compared to the west scan, i.e. the clearing scan. In the region of the hub height, i.e. about 130 m, tke is lower for the clearing scan which should be beneficial for wind turbines. The change when the terrain height is introduced is larger for the south compared to the west scan.

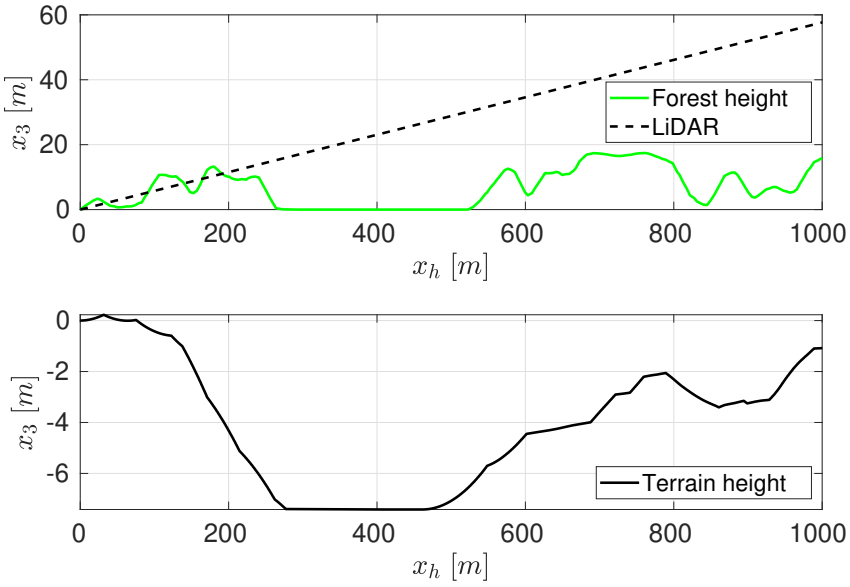

Figure 10. The top graph shows forest height and LiDAR height scan location for the west scan. The bottom graph displays the change in elevation.

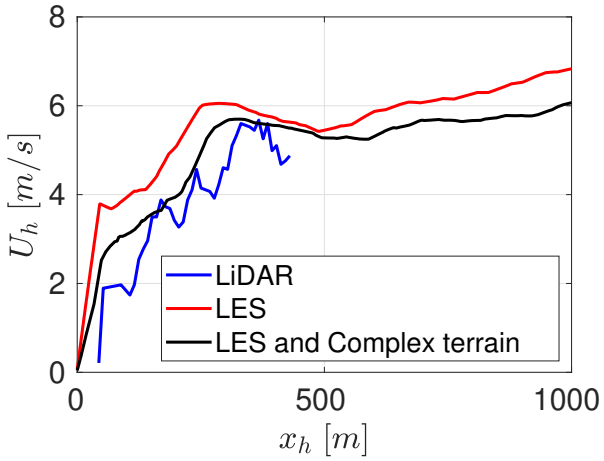

Figure 11. The horizontal wind speed of the flow above the clearing i.e. the west scan is displayed along the horizontal direction from the LiDAR location. The data is the same as shown in fig. 9 but displayed along the horizontal distance.

5. Conclusion

Measurements and simulation results show good agreement and taking the complex terrain into account improves the agreement even further. The uncertainty of the stratification of the measurements can be the reason for some of the difference, although the measurement were carried out during night time to increase the probability of neutral stratification. The vertical wind speed for the clearing scan change a lot when the complex terrain is taken into account. In the present work, the magnitudes of variation in terrain height are low. This shows the importance of including complex terrain for simulations with large change in elevation.

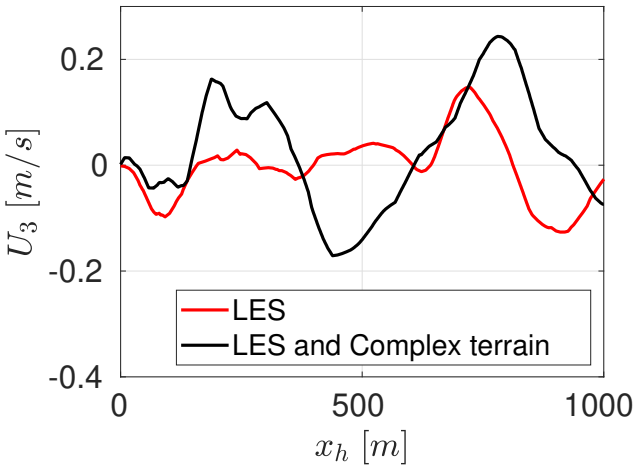

Figure 12. The vertical velocity of the wind for the west scan along the horizontal direction from the LiDAR location.

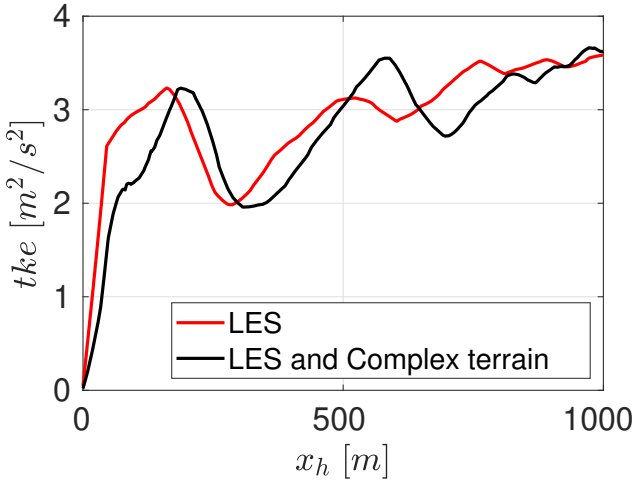

Figure 13. The resolved turbulent kinetic energy above the clearing displayed along the horizontal direction from the LiDAR location i.e. the x-axis.

When the normalized vertical profiles are compared, for the horizontal wind speed the effect of taking the complex terrain into account or not was largest for the forest scan. This is probably due to a somewhat larger change in elevation compared to the clearing scan. The shape of vertical wind speed changed the most for the clearing scan. The reason for this is probably the increase in elevation the 300 m from the wind turbine. But the magnitude of the normalized vertical velocity is small compared to the horizontal velocity.

The normalized turbulent kinetic energy is showing a decrease for the clearing scan compared to the forest scan which should be beneficial for wind turbines.

The impact of the wind farm about 2 km west is not investigated in the context of this article, but it could have a affect on the measurements for the west scan over the clearing.

Acknowledgments
This project is financed by the Swedish energy engency, Stena Renewable, Meventus and Vestas. The Lemnhult wind farm investigated in this article is owned by Stena Renewable. The LiDAR

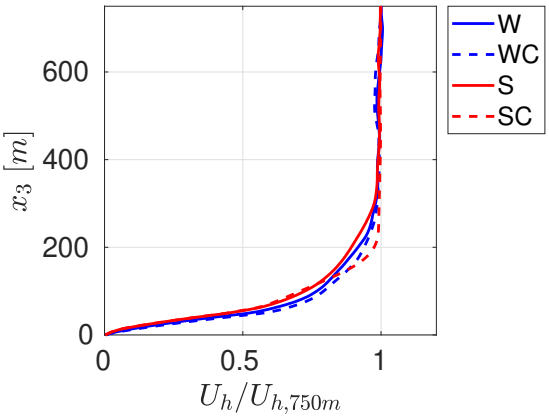

Figure 14. Horizontal velocities at the location of the LiDAR. W = West scan i.e. clearing scan, WC = West scan and complex terrain, S = South scan i.e. forest scan, SC = South scan and complex terrain.

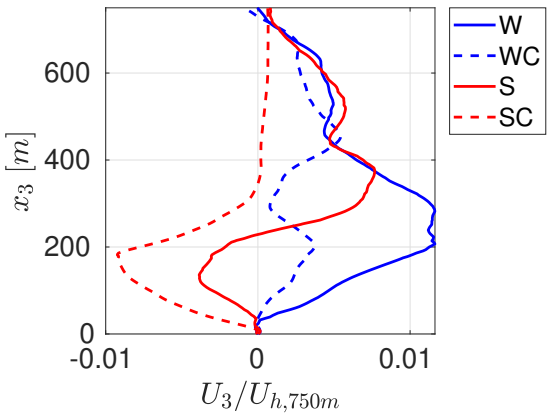

Figure 15. The vertical velocity at the location of the LiDAR. W = West scan i.e. clearing scan, WC = West scan and complex terrain, S = South scan i.e. forest scan, SC = South scan and complex terrain.

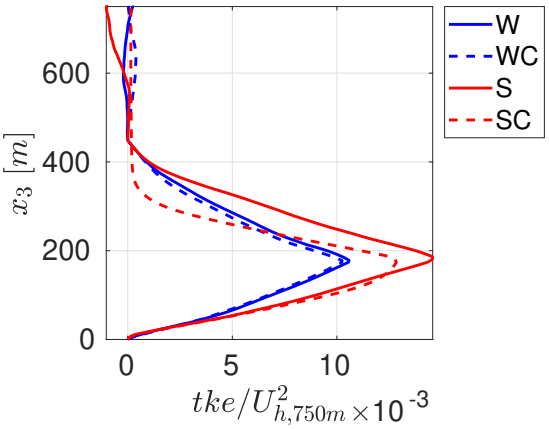

Figure 16. The turbulent kinetic energy at the location of the LiDAR. W = West scan i.e. clearing scan, WC = West scan and complex terrain, S = South scan i.e. forest scan, SC = South scan and complex terrain.

measurements where performed by Meventus. The computations were performed on resources provided by the Swedish National Infrastructure for Computing (SNIC) at C3SE partially funded by the Swedish Research Council.

References

[1] B. Nebenfuhr and L. Davidson. Influence of a forest canopy on the neutral atmospheric boundary layer a les study, 2014.
[2] M. Zendehbad, N. Chokani, and R. Abhari. Impact of forested fetch on energy yield and maintenance of wind turbines. *Renewable Energy*, 96:548–558, 2016.
[3] S. Dupont and Y. Brunet. Coherent structures in canopy edge flow: A large-eddy simulation study. *Journal of Fluid Mechanics*, 630(7):93–128, 2009.
[4] A. Sogachev, M. Leclrec, G. Zhang, U. Rannik, and T. Vesala. Co2 fluxes near a forest edge: A numerical study. *Ecological Application*, 18:1454–1469, 2008.

[5] F. Kanani-Subring and S. Raasch. Spatial variability of scalar concentrations and fluxes downstream of a clearing-to-forest transition: A large-eddy simulation study. *Boundary-Layer Meteorol*, 155:1–27, 2014.
[6] S. Dupont, J.-M. Bonnefond, M. R. Irvine, E. Lamaud, and Y. Brunet. Long-distance edge effects in a pine forest with a deep and sparse trunk space: In situ and numerical experiments. *Agricultural and Forest Meteorology*, 151(3):328–344, 2011.
[7] S. Dupont and Y. Brunet. Edge flow and canopy structure: A large-eddy simulation study. *Boundary-Layer Meteorology*, 126(1):51–71, 2008.
[8] J. Matsfelt. Large eddy simulation of clearings in forest and their effect on wind turbine. Thesis for licentiate of engineering, Div. of Fluid Dynamics, Dept. of Mechanics and Maritime Sciences, Chalmers University of Technology, Göteborg, Sweden, 2018.
[9] A. Glazunov and V. Stepanenko. Large-eddy simulation of stratified turbulent flows over heterogeneous landscapes. *Atmospheric and Oceanic Physics*, 51(4):403–415, 2015.
[10] S. Ivanell, J. Arnqvist, M. Avila, D. Cavar, R. Aurelio Chavez-Arroyo, H. Olivares-Espinosa, C. Peralta, J. Adib, and B. Witha. Microscale model comparison (benchmark) at the moderate complex forested site ryningsnäs. *Wind Energy Science Discussions*, 3:929–946, 2018.
[11] M. Mohr, J. Arnqvist, H. Abedi, H. Alfredsson, M. Baltscheffsky, H. Bergström, I. Carlen, L. Davidson, A. Segalini, and S. Soderberg. Wind power in forests ii. Vindforsk report, Uppsala University, 2018.
[12] F. Nicoud and F. Ducros. Subgrid-scale stress modelling based on the square of the velocity gradient tensor. *Flow, Turbulence and Combustion*, 62:183–200, 1999.
[13] R. Shaw and U. Shumann. Large-eddy simulation of turbulent flow above and within a forest. *Boundary-Layer Meteorology*, 61(1):47–64, 1992.
[14] B. Lalic and D. Mihailovic. An empirical relation describing leaf area density inside the forest for environmental modeling. *Journal of Applied Meteorology*, 43(4):641–645, 2004.
[15] N. Jarrin, S. Benhamadouche, D. Laurence, and R. Prosser. A synthetic-eddy-method for generating inflow conditions for large-eddy simulations. *International Journal of Heat and Fluid Flow*, 27:585–593, 2006.
[16] Lantmäteriet. Technical report, Lantmäteriet, Sweden, 2016.
[17] B. Nebenfuhr and L. Davidson. Large-eddy simulation study of thermally stratified canopy flow. *Boundary-Layer Meteorology*, 156(2):253–276, 2015.